Gapless excitations in the Haldane-Rezayi state: The thin-torus limit

Alexander Seidel and Kun Yang

Phys. Rev. B **84**, 085122 — Published 24 August 2011

DOI: 10.1103/PhysRevB.84.085122

Gapless excitations in the Haldane-Rezayi state: The thin torus limit

Alexander Seidel[1] and Kun Yang[2]

[1] *Department of Physics and Center for Materials Innovation, Washington University, St. Louis, MO 63136, USA*

[2] *National High Magnetic Field Laboratory, Florida State University, Tallahassee, Fl 32306, USA*

We study the thin torus limit of the Haldane-Rezayi state. Eight of the ten ground states are found to assume a simple product form in this limit, as is known to be the case for many other quantum Hall trial wave functions. The two remaining states have a somewhat unusual thin torus limit, where a "broken" pair of defects forming a singlet is completely delocalized. We derive these limits from the wave functions on the cylinder, and deduce the dominant matrix elements of the thin torus hollow-core Hamiltonian. We find that there are gapless excitations in the thin torus limit. This is in agreement with the expectation that local Hamiltonians stabilizing wave functions associated with non-unitary conformal field theories are gapless. We also use the thin torus analysis to obtain explicit counting formulas for the zero modes of the hollow-core Hamiltonian on the torus, as well as for the parent Hamiltonians of several other paired and related quantum Hall states.

I. INTRODUCTION

The theoretical study of electronic phases in the fractional quantum Hall regime owes much of its success to the construction of analytic trial wave functions,[1] and their subsequent interpretation in a conformal field theory (CFT) context.[2,3] The use of CFT gives rise to powerful predictions regarding, e.g., the edge physics of a state or its statistics. The connection between trial wave functions and CFT allows for elegant derivation of results without further microscopic studies of the wave functions themselves or their parent Hamiltonians. The use of CFT in this way is, however, not free of conjecture. One exciting development in the field is the gradual improvement of the foundation underlying these conjectures, e.g., regarding statistics.[4–7]

Another important prediction based on the CFT correspondence holds that wave functions related to non-unitary CFTs cannot be stabilized through local Hamiltonians with an energy gap in their bulk excitation spectrum.[5,6,8,9] In this paper we will show that this statement is consistent with a different scheme of attack recently found in the literature. This is to take the thin torus limit of a quantum Hall state, and assume adiabatic continuity between this quasi one-dimensional (1D) limit, and the limit of a two-dimensional (2D) torus without a "thin" dimension. Thus far, this method has been mainly used to study systems with a bulk energy gap.[10–13] Since early on, however, the assumption of adiabatic continuity has also been made for systems with gapless bulk excitations.[14] More recently we have applied[15] this method to a possible transition[16] between the Halperin (331)-state[17] and the Moore-Read state[2] triggered via interlayer tunneling. Here we apply the same approach to the Haldane-Rezayi state,[18] whose associated CFT is non-unitary.[2,19–21]

The thin torus approach is itself based on a conjecture, namely that of adiabatic continuity described above. The latter has led to some success in the past, but is so far less established overall compared to the CFT based conjecture. Since the assumptions underlying the thin torus method are, however, not field-theoretic in nature, they may be viewed as quite independent of those used in the CFT approach. It is thus reassuring that so far, the results of both approaches have been in overall agreement. This seems to include the issue of quasi-particles statistics.[22,23] The purpose of this paper is to demonstrate this agreement with regard to the existence of gapless excitations in the HR state. Furthermore, we use the insights gained from the thin torus limit to generalize various counting formulas,[24,25] which have been given for the zero energy modes of parent Hamiltonians in the case of spherical topology, to the torus. This is possible since in the thin torus limit, simple patterns generally appear that lead to combinatorial principles which organize the subspace of zero modes (cf. also Ref. 26). These patterns may also be viewed as dominance partitions of Jack polynomials,[27,28] and are related to "patterns of zeros".[29–31]

The paper is organized as follows. In Section II, we take the formal thin cylinder limit of HR wave functions on the cylinder. This allows us to infer all the patterns associated with topological sectors in the thin torus limit. In Section III we discuss the matrix elements of the thin torus hollow-core Hamiltonian, and use this to demonstrate the existence of gapless excitations in the thin torus limit. In Section IV we use the combinatorial principles imposed by the thin torus Hamiltonian to derive torus zero mode counting formulas for the HR state and various other paired and related quantum Hall states. We discuss our results in Section V. Various technicalities relating to the thin torus limit are presented in three Appendices.

II. THE THIN TORUS LIMIT

A. Preliminary considerations

We focus on the Haldane-Rezayi (HR) state at filling factor $\nu = 1/2$. This is the top state in the HR sequence, and is its most elementary state in terms of torus degeneracy. Even so, for even particle number, its torus degeneracy of 10 of this state is already rather large. The corresponding torus wave functions have been constructed in Refs. 24 and 32. The full set of patterns associated with these states have been known for some time,[33,34] and naturally appear when the thin torus limit is taken. In this limit, trial wave functions for ground states usually approach simple product states,[35] and patterns appear as patterns of occupancy numbers of consecutive lowest landau level (LLL) orbitals. For the 10 HR ground states, eight of the associated patterns are easy to guess. The particles in the associated product state carry a spin or pseudo-spin label, and must form a singlet, since the HR state is a two-component singlet state. A simple pattern, that is, one with a simple unit cell, must therefore contain at least two particles per unit cell that form a singlet. Natural candidates are thus given by the following patterns

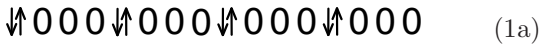
(1a)


(1b)

Here as usual, patterns denote consecutive occupancies of LLL orbitals in the thin torus limit, and ovals denote singlets formed by two electrons in different orbitals. Taking into account translational symmetry on the torus, these patterns together account for eight degenerate ground state. They have also appeared in the literature more recently from a "generalized Pauli principle" point of view[36,37] (cf. also Ref. 38). The above, however, leaves the thin torus limits of two more ground states undetermined, and the associated patterns have to our knowledge not yet appeared in the printed literature.[33,34] Interestingly, these patterns are not "simple", in the sense that they are not described by a small unit cell. Indeed, since any such unit cell must harbor at least two particles in a singlet state, and hence must at least consist of four LLL orbitals at $\nu = 1/2$, any such patter would imply the existence of four more ground state. It is therefore not possible that the thin torus limit of the remaining two ground states yields a pattern with a simple unit cell. In fact, as we will show below, it is the existence of these two rather "special" ground state sectors which implies the existence of gapless excitations in the state, at least in the thin torus limit.

B. The A pattern

We proceed by first deriving the thin torus limits of Eq. (1) in a systematic way, by following the general method developed earlier by us.[15] In this method, the thin torus pattern is first obtained on a "squeezed lattice", and then unsqueezed by well defined rules. Here we give a self-contained account of this method, including some details not explicit in the original work.

Since torus wave functions are generally complicated and lack a simple polynomial structure, we use the fact that all torus patterns can also be obtained by working on the cylinder with appropriate "boundary conditions", corresponding to various edge state configurations (vacua) (cf. Ref. 15). We will demonstrate this as we go along. To begin, we take the polynomial structure associated with the HR ground state in planar or spherical geometry,[18] and write down a corresponding LLL state on the cylinder:

$$H_A(\{\xi_\alpha\}) = \sum_{\sigma\in S_{N/2}} \frac{(-1)^\sigma}{(\xi_{1\downarrow}-\xi_{\sigma_1\uparrow})^2\ldots(\xi_{\frac{N}{2}\downarrow}-\xi_{\sigma_{\frac{N}{2}}\uparrow})^2} \times \prod_{\alpha<\beta}(\xi_\alpha-\xi_\beta)^2\,. \tag{2}$$

Here, $\xi_\alpha = \exp(\kappa(x_\alpha + iy_\alpha))$, $\kappa = 2\pi/L_y$ is the inverse radius of the cylinder, greek letters are multi-indices of the form $\alpha = (i, S_z)$, referring to the $i-th$ particle with spin projection $S_z =\uparrow$ or $S_z =\downarrow$, and $\alpha < \beta$ refers, for definiteness, to the lexicographic order $(1,\downarrow) < \ldots < (N/2,\downarrow) < (1,\uparrow) < \ldots < (N/2,\uparrow)$. There are $N/2$ particles for each projection. The structure of Eq. (2) has the familiar form of a Laughlin-Jastrow factor multiplied by a determinant, which we have written out explicitly. We suppress the standard Gaussian factor $\exp(-\frac{1}{2}\sum_\alpha x_\alpha^2)$ here and in the following.

One can now imagine expanding Eq. (2) into polynomials of the form $\prod_\alpha \xi_\alpha^{n_\alpha}$. Let $C_{\{n_\alpha\}}$ be the coefficient of such a monomial. This coefficient is essentially the amplitude $A_{\{n_\alpha\}}$ for the product state that has particles occupying the LLL orbitals $\{n_\alpha\}$, except for a normalization factor:[35]

$$A_{\{n_\alpha\}} = e^{\frac{1}{2}\kappa^2 S}\, C_{\{n_\alpha\}}\,, \tag{3}$$

where

$$S = \sum_\alpha n_\alpha^2\,. \tag{4}$$

For this reason, those product states will dominate the thin cylinder limit $\kappa\to\infty$ for which the quantity S takes on the maximum value, subject to the constraint that the associated polynomial coefficients $C_{\{n_\alpha\}}$ are non-zero. The n_α in any monomial with non-zero coefficient are of the following form:

$$n_\alpha = \sum_{\beta\neq\alpha}(m_{\alpha\beta} + p_{\alpha\beta}) \tag{5}$$

where $m_{\alpha\beta}$ and $p_{\alpha\beta}$ are symmetric and anti-symmetric matrices, respectively, that correspond to the selection of the term $\xi_\alpha^{m_{\alpha\beta}+p_{\alpha\beta}}\ \xi_\beta^{m_{\alpha\beta}-p_{\alpha\beta}}$ in a factor depending on

ξ_α and ξ_β in Eq. (2). In the present case, all factors surviving cancellation are of the form $(\xi_\alpha - \xi_\beta)^2$. For these terms, $m_{\alpha\beta} = 1$ and $p_{\alpha\beta} \in \{-1, 0, 1\}$. For a fixed permutation σ, however, factors corresponding to certain pairs $(\alpha\beta)$ in the Laughlin-Jastrow factor are canceled, and this imposes additional constraints on $m_{\alpha\beta}$ and $p_{\alpha\beta}$. More precisely,

$$\begin{aligned} &m_{\alpha\beta} = 0 \text{ for } \alpha = \beta \\ &m_{\alpha\beta} = 0 \text{ for } (\alpha, \beta) \in \{(i\downarrow, \sigma_i\uparrow) : i = 1 \dots N/2\} \\ &m_{\alpha\beta} = 1 \text{ otherwise.} \end{aligned} \tag{6}$$

where $(\cdot, \cdot)$ denotes an unordered pair, and

$$p_{\alpha\beta} \ \in \{-m_{\alpha\beta}, -m_{\alpha\beta} + 1 \dots m_{\alpha\beta}\} \ . \tag{7}$$

A given permutation σ thus induces a pairing between up-spins and down-spins, which determines the possible monomials $\prod_\alpha \xi_\alpha^{n_\alpha}$ through the rules (5)-(7). In addition, $p_{\alpha\beta}$ is constrained by its anti-symmetry. Making all possible choices for $p_{\alpha\beta}$ generates all possible monomials for given a given pairing σ. In Appendix A, we show that in order to maximize Eq. (4), $p_{\alpha\beta}$ must be of the following form,

$$p_{\alpha\beta} \ = m_{\alpha\beta} \operatorname{sign}(\rho_\alpha - \rho_\beta), \tag{8}$$

where $\rho \in S_N$ is a permutation of N objects. This means that $|p_{\alpha\beta}|$ must always be chosen to have its maximum possible value, $m_{\alpha\beta}$, and the sign structure is determined by an ordering of the particle indices. Eq. (8) implies that in each factor $(\xi_\alpha - \xi_\beta)^2$, we pick either the term ξ_α^2 or the term ξ_β^2, as determined by ρ, but never the mixed term. ρ may be thought of as determining the order of the N-particles on a "squeezed" lattice of N sites. The term "squeezed" implies that the arrangement of the particles on the squeezed lattices is a precursor of the thin cylinder pattern we seek, but with all inter-particle distances set equal to 1 (hence, with vacant sites "squeezed out"). The corresponding un-squeezed pattern, the thin cylinder limit of the state, is then obtained by evaluating Eq. (5) for given $p_{\alpha\beta}$ and $m_{\alpha\beta}$, as determined by σ, ρ via Eqs. (6), (8). The resulting n_α determine the exponents in a dominant monomial $\prod_\alpha \xi_\alpha^{n_\alpha}$, which corresponds to a product state where the particle with index α occupies the LLL orbital with index n_α.

In the above, the choice of the pairing σ is arbitrary, since varying σ only anti-symmetrizes the resulting monomials. We may thus choose $\sigma = id$ without loss of generality. However, for given σ, the proper choice of ρ that maximizes Eq. (4) is not arbitrary. Rather, to determine the proper arrangement of particles on the squeezed lattice, we must minimize an effective energy, as done in Appendix B. This yields that for $\sigma = id$, a proper choice of ρ is

$$\rho = 1\downarrow, 1\uparrow, 2\downarrow, 2\uparrow, \dots, \frac{N}{2}\downarrow, \frac{N}{2}\uparrow \ . \tag{9}$$

I.e., the particles paired according to σ must be neighbors on the squeezed lattice. Permuting neighboring up- and downspin particles with the same particle index results in the same p-matrix, since $p_{\alpha\beta} \ = 0$ for the corresponding multi-indices α, β. We may of course permute the overall order of pairs, where different orders leads to different monomials contributing to the single Slater determinant that dominates the thin cylinder limit. Using Eq. (9) in Eq. (5), the resulting values n_α then are, listed in the order given by the right hand side of Eq. (9):

$$n_\alpha = 0, 0, 4, 4, 8, 8, \dots \tag{10}$$

When the corresponding spins are distributed over LLL orbitals accordingly, this yields the pattern Eq. (1a). It follows from the above that each monomial that is present in the associated Slater determinant is obtained from one and only one choice for the p-matrix.[39] The corresponding monomial is hence generated in only one way, and is thus guaranteed to have a non-zero coefficient.

C. The B patterns

The N-particle ground state on an infinite cylinder is infinitely degenerate by translational symmetry. However, valid incompressible ground state wave functions come in a finite number of different classes, corresponding to the different patterns obtained when taking the thin cylinder limit. To obtain a different class of ground state, we may use the following procedure. The state (2) describes a "ribbon" of incompressible fluid with two opposing edges.[35] Inside this ribbon, we can make two quasi-hole type excitations Fig. (1). One member of the pair is then formally taken across the left edge to $x = -\infty$, whereas the other is taken across the right edge to $x = +\infty$. With the holes removed, the state has healed into an incompressible fluid, but in a different ground state sector not (necessarily) related to the original one by translation. On the sphere, the same process corresponds to placing the two members of the quasi-hole pair at the north and south pole, respectively. We may thus take the polynomials associated with quasi-hole wave functions from work done in spherical geometry.[24] Recall that the polynomial (2) corresponds to the unique ground state on the sphere. As observed in Ref. 24, there is only one class of two-quasi-hole states that can be generated inside this ground state, whereas for $2n$-holes with $n > 1$, various classes (sectors) can be distinguished due to additional degrees of freedom corresponding to pair breaking. We will find a natural interpretation for this behavior in the quasi 1D. We take the unique class of polynomial wave functions describing two quasi-holes generated in the ground state (2), parameterized by the two quasi-hole coordinates h_1 and h_2, and take the limits described above. The resulting ground state polynomial

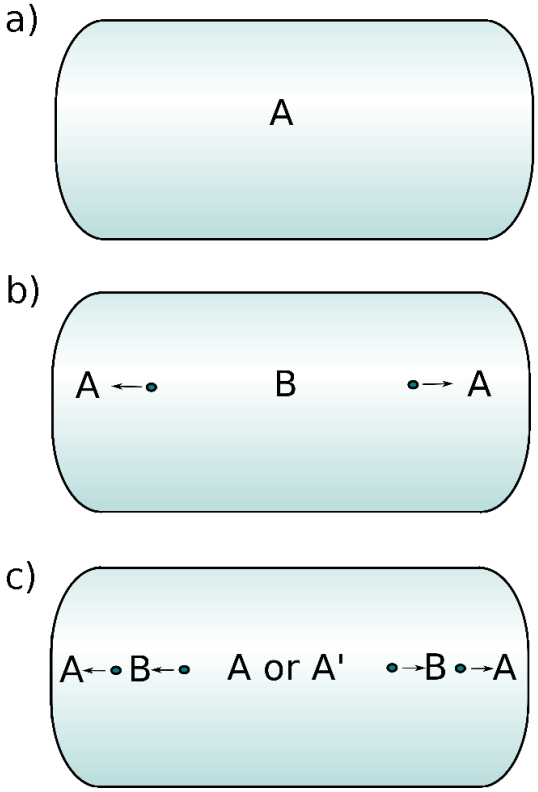

FIG. 1. Transitions between different ground state sectors of the HR state by quasi-hole insertion. We start with the polynomial Eq. (2), which corresponds to the unique ground state on the sphere, and consider the associated state on the cylinder (a). The thin cylinder limit of this state is given by the A pattern, Eq. (1a). Insertion of two quasi-holes (b) leads to a state whose thin cylinder limit is shown in Fig. 4a), with a B pattern appearing inside the A pattern, and separated from it by two domain walls. When the quasi-hole positions are taken to $\pm\infty$, the state approaches Eq. (11), whose thin cylinder limit is described by the B pattern (1b). We may iterate the process by inserting a second quasi-hole pair (c). For this one has the choice of breaking a pair in the pairing wave function of the state, or not.[24] In the latter case, another A-pattern will appear in the thin cylinder limit, surrounded by B-patterns. If, on the other hand, the pair is broken, one obtains an "A'-string" instead. With the quasi-holes taken to $\pm\infty$, the state approached the wave function Eq. (16). Its thin cylinder limit is the superposition of states represented in Fig. 2, which features a delocalized broken pair, and which we will loosely refer to as an A'-string. (See also Fig. 4e) for the appearance of an A'-string terminating in domain walls before quasi-holes are taken to $\pm\infty$.)

is then

$$H_B(\{\xi_\alpha\}) = \sum_{\sigma\in S_{N/2}} \frac{(-1)^\sigma(\xi_{1\downarrow}+\xi_{\sigma_1\uparrow})\dots(\xi_{\frac{N}{2}\downarrow}+\xi_{\sigma_{\frac{N}{2}}\uparrow})}{(\xi_{1\downarrow}-\xi_{\sigma_1\uparrow})^2\dots(\xi_{\frac{N}{2}\downarrow}-\xi_{\sigma_{\frac{N}{2}}\uparrow})^2} \times \prod_{\alpha<\beta}(\xi_\alpha-\xi_\beta)^2 . \tag{11}$$

It is not difficult to see that, like H_A, H_B has the analytic properties that render it a zero-energy eigenstate of the hollow-core Hamiltonian.[18,24] The fact that H_B describes an incompressible state at the same filling factor as H_A will be apparent in the thin cylinder limit.

It remains to see how the rules of the game described above to find the dominant thin cylinder monomials of H_A change for the polynomial H_B. This is easy to see that only the central line of Eq. (6) needs modification:

$$m_{\alpha\beta} = 1/2, \text{ for } (\alpha,\beta)\in\{(i\downarrow,\sigma_i\uparrow) : i = 1\dots N/2\} . \tag{12}$$

The change just describes the following fact: Now terms in the Laughlin-Jastrow factor that belong to the pairing associated with σ are not just canceled, but are replaced by $(\xi_\alpha+\xi_\beta)$. For the reasons described above, we can look at $\sigma = id$ without loss of generality. Eq. (9) is then still a solution for ρ that maximizes S, Eq. (4) (Appendix B). The resulting monomial corresponds to the product state

$$\downarrow\uparrow 0\,0\downarrow\uparrow 0\,0\downarrow\uparrow 0\,0\downarrow\uparrow 0\,0\downarrow\uparrow \tag{13}$$

However, permuting the order of a pair $i\uparrow, i\downarrow$ in ρ, Eq. (9), now leads to a different $p_{\alpha\beta}$ that also maximizes S, with the members of the i-th pair in Eq. (13) trading places. It follows that the dominant state in the thin cylinder limit is an equal amplitude superposition of all states generated from Eq. (13) by exchanging the opposite spins of neighboring pairs in a possible ways. It is worth checking that the signs work out for this state to describe a product of singlets, as shown in Eq. (1b). For this it is enough to consider a state with $N = 2$ particles. According to the above, the dominant term in the thin cylinder limit is:

$$\xi^0_\alpha\xi^1_\beta + \xi^1_\alpha\xi^0_\beta = \xi_\alpha+\xi_\beta . \tag{14}$$

Here, α and β refer to the down-spin particle and the up-spin particle, respectively. In writing down the wave functions (2), (11), we have distinguished two subspecies of opposite spin, and have not imposed any anti-symmetry condition between these distinguishable subspecies. Rather, in Eq. (14) α is always associated with a down-spin particle, and β is always associated with an up-spin particle. Viewed as a function of position *and* spin coordinates, Eq. (14) should be multiplied with the spinor $\delta_{s_\alpha,\downarrow}\delta_{s_\beta,\uparrow}$. The fully anti-symmetrized wave function is then

$$(\xi_\alpha\delta_{s_\alpha,\downarrow}\delta_{s_\beta,\uparrow}-\xi_\beta\delta_{s_\alpha,\uparrow}\delta_{s_\beta,\downarrow})-(\xi_\alpha\delta_{s_\alpha,\uparrow}\delta_{s_\beta,\downarrow}-\xi_\beta\delta_{s_\alpha,\downarrow}\delta_{s_\beta,\uparrow}) \tag{15}$$

This is easily seen to be the difference between two Slater determinants, describing a singlet. Hence, despite the seeming lack of anti-symmetry, Eq. (14) describes a singlet, and we recover the pattern Eq. (1b) in the thin cylinder limit of Eq. (11). The fact that the common coefficient of the dominant monomials obtained here is non-zero follows from observations similar to those made at the end of the preceding section.

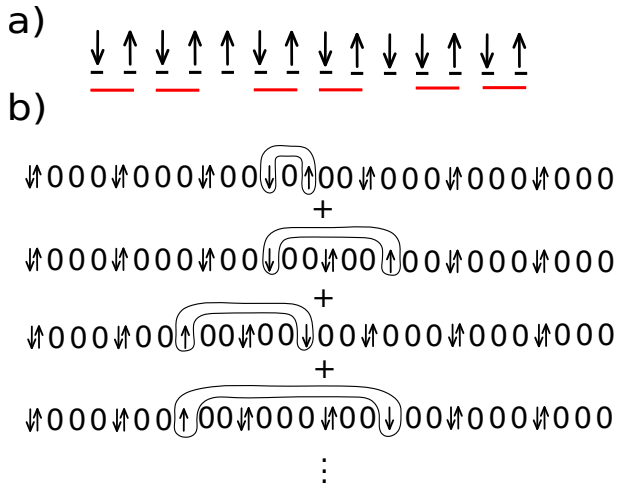

FIG. 2. The thin cylinder limit of the A' ground state, Eq. (16). (a) One of many squeezed lattice configurations, corresponding to a choice of the permutation ρ that maximizes the quantity S, Eq. (4). A particular choice of ρ corresponds to a squeezed lattice configuration where each spin carries a particle number index. This is not shown, since permutation of like-spin indices does not change the value of S, as it must be by the anti-symmetry of the wave function. The short underscores represent squeezed lattice sites, and the long underscores indicate the pairing $\mathcal{P}$, Eq. (23). Pairs must be nearest neighbors on the squeezed lattice, whereas the positions of the members of the broken pair are arbitrary. Together, ρ and $\mathcal{P}$ completely define the p-matrix, Eq. (22). (b) The thin cylinder limit of the A'-state, obtained as equal amplitude superposition of all product states derived by unsqueezing all squeezed lattice configurations with given pairings of the form described under (a). This is done by using the associated p-matrix described in (a) to form monomials according to Eqs. (18), (5). The unsqueezed version of (a) is shown in the last line. As a result, the state is one where a completely *delocalized* pair of charge neutral defects forming a singlet separates two mutually out-of-phase A-patterns.

D. The A' pattern

The missing ground state sectors can be obtained by iterating the above procedure. We thus create two more quasi-holes in the state (11). The number of inequivalent choices for this is the number of inequivalent choices to make four quasi-holes in the original ground state (2), which is in one-to-one correspondence with the ground state on the sphere. For this it was found in Ref. 24 that there are two such possibilities, One may be described as having a "broken pair", while the other does not. In the latter case, after sending both quasi-hole pairs off to $\pm\infty$, we obtain a state whose thin cylinder limit is again of the A-type, Eq. (1a). Hence we focus on the former case, where the state has a broken pair. The analytic form of these states is more complicated, especially so on the torus.[24,32] On the cylinder, again after sending the members of each pair to $\pm\infty$, we obtain the following wave function:

$$H_C(\{\xi_\alpha\}) = \sum_{\sigma\in S_{N/2}} \sum_{\lambda\in S_{N/2}} (-1)^\sigma (-1)^\lambda \prod_{i=2}^{N/2} \frac{(\xi_{\sigma_i\downarrow} + \xi_{\lambda_i\uparrow})^2}{(\xi_{\sigma_i\downarrow} - \xi_{\lambda_i\uparrow})^2} \times \prod_{\alpha<\beta} (\xi_\alpha - \xi_\beta)^2 \,. \tag{16}$$

In the above expression, the pairing between up-spin and down-spin particles is now facilitated two permutations λ and σ. The pairs thus formed are of the form $(\sigma_i\downarrow, \lambda_i\uparrow)$, where the pair with index $i = 1$ does not appear in the pairing factor of the state, and can hence be thought of as "broken". The thin cylinder analysis is seemingly simple. In Eq. (16), the summand corresponding to a fixed pairing σ, λ is of the form

$$\prod_{\alpha<\beta} (\xi_\alpha \pm \xi_\beta)^2 \,, \tag{17}$$

where in each factor, the sign depends on α, β and the pairing. The dominant monomials in such a term are the same as those in a pure Laughlin-Jastrow factor. Namely, the problem of finding the dominant monomial in the above product again reduces to Eq. (5), this time with

$$m_{\alpha\beta} = 1 - \delta_{\alpha\beta} \tag{18}$$

(all factors in the product are homogeneous and of the same order). The analysis given above again implies that the dominant monomials of Eq. (17) never make use of the mixed term in $(\xi_\alpha \pm \xi_\beta)^2$. These monomials would give rise to states where every second LLL-orbital is occupied, in all possible ways. However, the monomials thus generated do not depend on the permutations λ, σ at all, since only the mixed term in $(\xi_\alpha \pm \xi_\beta)^2$ depends on the latter. It is thus clear that in the sum over λ, σ in Eq. (16), all these naively dominant monomials cancel.

We thus have to look for those monomials in Eq. (17) with the largest value of S, Eq. (4), whose coefficient remains non-zero after the sum over λ, σ is taken in Eq. (16). Note that, since λ, σ only affect the signs in Eq. (17), the possible range of values for $p_{\alpha\beta}$ is always $\{-1, 0, 1\}$, independent of α, β. Each choice for $p_{\alpha\beta}$ corresponds to the choice of the term proportional to $\xi_\alpha^{1+p_{\alpha\beta}}\ \xi_\beta^{1-p_{\alpha\beta}}$ in the factor $(\xi_\alpha \pm \xi_\beta)^2$. It is thus useful to think of Eq. (16) in terms of two *independent* sums:

$$H_C(\{\xi_\alpha\}) = \sum_{\{p_{\alpha\beta}\}} \prod_{\alpha<\beta} \xi_\alpha^{1+p_{\alpha\beta}}\ \xi_\beta^{1-p_{\alpha\beta}} \times \sum_{\sigma,\lambda\in S_{N/2}} (-1)^\sigma (-1)^\lambda \mathrm{coeff}(\lambda, \sigma, \{p_{\alpha\beta}\}) \tag{19}$$

The problem is thus to choose $p_{\alpha\beta}$ such that Eq. (4) is maximized, subject to the constraint that the second row in the above equation does not vanish.[40] Suppose, now,

that $p_{\alpha\beta}$ is such that for the i-th down-spin particle, we have

$$p_{i\downarrow,\beta} = -p_{\beta,i\downarrow} = \pm 1 \text{ for all } \beta \,. \tag{20}$$

We will now show that there can be only one such i in order for the sum over coefficients in Eq. (19) not to vanish. If there were two indices i_1 and i_2 that satisfy Eq. (20), then exchanging the positions $\sigma^{-1}(i_{1,2})$ of these two indices in the permutation σ changes the sign $(-1)^\sigma$, but leave the coefficient coeff$(\sigma, \lambda, \{p_{\alpha\beta}\})$ unchanged. This is so because this coefficient can depend on $\sigma^{-1}(i)$, only through the mixed term in $(\xi_{i\downarrow} \pm \xi_\beta)^2$ (whose sign depends on whether $\beta = (\lambda_{\sigma^{-1}(i)}, \uparrow)$ or not), but for i_1, i_2 satisfying (20), these mixed terms do not enter the monomial associated with $p_{\alpha\beta}$. Therefore, we can have at most one down-spin index i satisfying (20). For the same reasons there can be at most one up-spin index j with

$$p_{j\uparrow,\beta} = -p_{\beta,j\uparrow} = \pm 1 \text{ for all } \beta \,. \tag{21}$$

When $p_{\alpha\beta}$ is subject to the additional constraint that at most one i and one j satisfy (20) and (21), respectively, we can still use the arguments of Appendix A to show that the $p_{\alpha\beta}$ maximizing Eq. (4) is of the form

$$p_{\alpha\beta} \ = s_{\alpha\beta}\, \mathrm{sign}(\rho_\alpha - \rho_\beta), \tag{22}$$

for some permutation ρ, only we cannot always choose the maximum value $m_{\alpha\beta} = 1$ for $|p_{\alpha\beta}| = s_{\alpha\beta}$ any more. We will, however, still want to choose $s_{\alpha\beta} = 1$ as often as possible, in order to approach the unconstrained maximum value of S as closely as possible. To do this, we choose one index $(i\downarrow)$ and one index $(j\uparrow)$ for which (20) and (21) will be satisfied. The remaining $N-2$ particle indices are organized into a pairing $\mathcal{P} = \{(\alpha,\beta)\}$ (*different* from the pairing induced by σ and λ), each pair consisting of an up-spin and a down-spin index. We then define

$$\begin{aligned} &s_{\alpha\beta} = 0 \text{ if } \alpha = \beta \text{ or } (\alpha,\beta) \in \mathcal{P} \\ &s_{\alpha\beta} = 1 \text{ otherwise} \end{aligned} \tag{23}$$

It is clear that this assigns a minimum number of off-diagonal zeros to the s-matrix, subject to the constraints described above. In any monomial obtained from Eqs. (22), (23), the indices $(i\downarrow)$ and $(j\uparrow)$ indeed play the role of a "broken pair", since no term coming from a factor $(\xi_{i\downarrow} \pm \xi_\beta)^2$ or $(\xi_{j\uparrow} \pm \xi_\beta)^2$ is ever affected by the relative sign that comes from the pairing wave function.

The permutation ρ that leads to a maximum value of S is not arbitrary, but its proper choice depends somewhat on the pairing $\mathcal{P}$. Again, we consider ρ to define a squeezed lattice configuration as described above. Then, as we show in Appendix B, we must arrange the pairs in $\mathcal{P}$ as nearest neighbors on the squeezed lattice. The location of the members of the broken pair is, however, arbitrary. This leads to the possible squeezed lattice configurations of the kind shown shown in Fig. 2a). The corresponding unsqueezed configurations, obtained by plugging the result into Eq. (5), is shown in Fig. 2b) (last line). As shown in the figure, there are still many other different degenerate configurations, corresponding to all possible positions of the members of the broken pairs. The term dominating the thin cylinder limit of Eq. (16) is an equal amplitude superposition of all the corresponding monomials. In Appendix C, we evaluate the coefficient of these monomials to be $2^{N-2}(N/2-1)!$, up to a sign, showing in particular that it is non-zero. Moreover, the superposition is symmetric in the positions of the members of the broken pair. By the same argument given at the end of the preceding section, this implies that this broken pair forms a singlet, as it should. The members of the remaining, unbroken pairs each occupy the same orbital, and thus form singlets automatically.

As is clear from the graphical representation in Fig. 2b), the thin cylinder limit of Eq. (16) is a equal amplitude superposition of all states where a delocalized singlet separates two mutually out-of-phase A-patterns. More precisely, the A-patterns thus separated differ by a shift of two orbitals. On the torus, there are exactly two such states, related by a single translation. Indeed, one will easily see that translating the state displayed in Fig. 2b) by *two* orbitals leaves the state invariant, whereas a single translation leads to the appearance of the other pair out of the four possible A-patterns, separated by defects. We will henceforth refer to these thin torus/cylinder states as A'-states or -patterns. It is natural to think of these states not as defining new topological sectors, but as A-type states in the presence of a single "zero-energy excitation." We further elaborate on this notion in the following section.

III. PROPERTIES OF THE THIN TORUS HOLLOW-CORE HAMILTONIAN: MATRIX ELEMENTS AND GAPLESS EXCITATIONS

This section presents the case for gapless excitations in the thin torus limit. It details the logic behind results first given in Refs. 33 and 34. The central step is the correct extraction of the dominant matrix elements of the hollow-core Hamiltonian in the thin torus limit. The diagonal parts of these matrix elements give rise to what has more recently been proposed as a "generalized Pauli principle" applying to the HR state.[37] We find it crucial, however, to also pay attention to off-diagonal matrix elements that survive in this limit. This then implies existence of of gapless modes in the thin torus limit. Our results will also allow us to derive a detailed formula for the number of zero energy eigenstates, or "zero modes", of the hollow-core Hamiltonian on the torus in the presence of quasi-holes.

It is well known that the analytic properties of the HR-states render them unique zero-energy ground states of the hollow-core Hamiltonian.[18] At filling factor $\nu = 1/2$, there are ten such ground states on the torus,[24,32] irrespective of the aspect ratio of the torus. In the thin torus limit, these ten ground states evolve into product

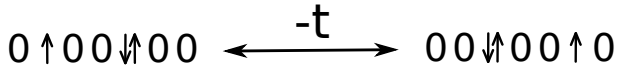

FIG. 3. The off-diagonal matrix element present in the thin torus hollow-core Hamiltonian. This, together with the "detailed balance" condition Eq. (24), ensures that states containing A'-type string with one or two delocalized defects are zero energy states in the thin torus limit.

states corresponding to the patterns that we have seen to emerge in the thin cylinder limit. Indeed, when expressed as a second-quantized Hamiltonian in the LLL-basis, the hollow-core Hamiltonian will be dominated by highly local terms, with sub-dominant terms exponentially suppressed (cf., e.g., Ref. 10). These dominant terms are identical in the case of a thin cylinder and a thin torus, for a given size (perimeter) of the small dimension. In general, the extraction of the proper dominant terms, which directly imply the thin torus limiting states, requires the use of degenerate perturbation theory, as we described earlier.[15] Here we pursue a shortcut instead. The dominant terms of the thin torus Hamiltonian follow quite unequivocally from the knowledge of the limiting zero-energy ground states, and the fact that the limiting Hamiltonian is local, with terms decaying exponentially with distance. This decay happens over a characteristic scale that is *short* compared to the orbital separation. The latter essentially implies that no two terms can compete (lead to cancellations in the ground state energy) that act at a different range. This imposes severe constraints on the effective thin torus Hamiltonian.

Considering the A- and B- ground states, clearly there must be terms in the thin torus Hamiltonian that assign an energy to any four adjacent orbitals containing more than two particles, or else there would be zero modes at higher filling factor. Likewise, there must be an energy cost associated with any two particles that are no more than two orbitals apart, *if* these two particles are forming a triplet. There is no such energy cost for singlets. Without this triplet energy, we could make many $\nu = 1/2$ zero modes by placing one particle of any spin orientation in every second orbital. In the presence of only these two types of interactions, the A- and B-type product states would be the unique zero energy ground states at filling factor $\nu = 1/2$. To allow for the A'-type states, off-diagonal terms of competitive magnitude must also be present. These terms will act on configurations where a doubly occupied orbital and a singly occupied orbital are separated by two empty sites, Fig. 3. The off-diagonal matrix element leads to a new configuration where the doubly occupied site and the single particle have moved past one another, essentially trading places while conserving their center-of-mass. We denote the strength of this matrix element by $-t$. At the same time, since the particle configuration described here involves three particles in four adjacent sites, there must be an energy cost V associated with it. It is easy to see that for

$$V = t \,, \tag{24}$$

the A'-pattern is a zero energy eigenstate of the resulting Hamiltonian. To see this, we first discuss the case of odd particle number. Indeed, the matrix elements defined above immediately imply that there must also be zero energy states for N odd,[24] in the thin torus limit. In this limit, these states are equal amplitude superpositions of all states connected by the off-diagonal matrix element described above, where a singly occupied orbital forms a defect between two adjacent A-patterns, and becomes delocalized my means of the process shown in Fig. 3. It is easy to see that for a given spin state of the defect site, there are two classes of states connected by such matrix elements. This gives rise to two ground states for each value of S_z, related by a single magnetic translation. The fact that the equal amplitude superpositions of this kind are zero energy eigenstates of the Hamiltonian defined above can be understood as a consequence of a "detailed balance" condition: Consider a state entering the superposition, with the defect in a fixed position. The diagonal energy associated with this state ($2t$) equals t times the number of other such states (2) that have direct matrix element with the state under consideration. Note that the diagonal energy is indeed $2t$, because of the doubly occupied orbitals to the left and right of the defect. General solvable Hamiltonians satisfying detailed balance conditions have been studied in Ref. 41.

The above considerations immediately extend to the A'-type states for even particle number. Now each state in the equal amplitude superposition has two defects, which form a singlet. We see that the detailed balance condition is still satisfied. The only states in the superposition that require additional consideration are those where the two defects are near neighbors, as in the first line of Fig. 2b). In this configuration, the diagonal energy cost is reduced by half, since each defect sees only one neighboring doubly occupied site, three orbitals away. The other neighbor is given by the other defect, two sites away. However, as stated above, two particles forming a singlet do not repel each other, even at close distance. The energy of the state is thus again $2t$. On the other hand, there are only two other configurations (as opposed to four) with direct matrix elements into this state.

We see now that the above matrix elements lead to the known thin torus ground states. Interestingly, however, they also imply the existence of gapless excitations in the thin torus limit. This can be seen in two different ways. First, we can consider an equal amplitude superposition like the A'-states, but with the defect pair put into a triplet state. This will lead to a new orthogonal state with a finite energy expectation value. However, this energy will vanish in the thermodynamic limit, since the amplitude of each configuration scales as $1/N$, and the number of offensive configurations scales as N, leading to an energy expectation value of order t/N.

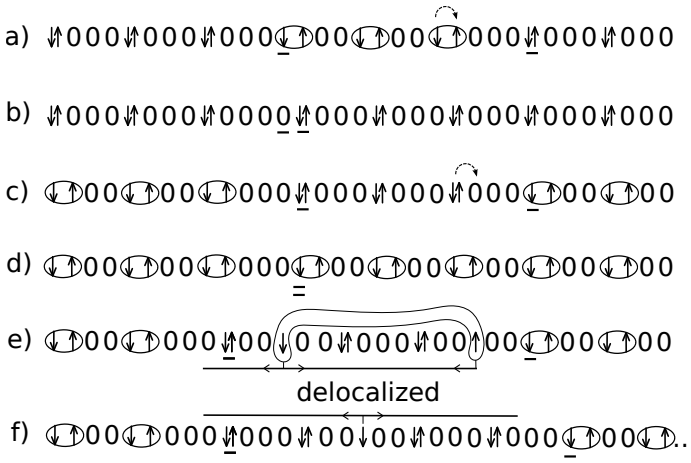

FIG. 4. Charge 1/4 Domain walls between A/A' and B-strings. Underscores label the domain wall positions as defined in the text. The hopping process indicated in a) moves the right domain wall in the ABA sequence to the left by four orbitals. b) shows the situation after three such moves, which shrinks the size of the B-string to zero, and leads to an additional 0 between mutually shifted A-strings. c)+d) shows the same for a BAB sequence. Note that for the conventions defined in the text, the merged domain walls now coincide at the same orbital. In any case, each allowed zero energy sequence of patterns can be assigned a sequence of domain wall positions satisfying Eq. (28) in a unique manner. e) and f) show patterns involving A'-strings with two (e) or one (f) delocalized defect. Only a "snapshot" of the state is shown with defects in fixed positions, where it is understood that these defects are delocalized as indicated and stated in the text. The right defect in (e) is shown at the rightmost possible position.

Moreover, we can also consider giving the delocalized singlet defect in the A'-state a small but finite momentum k. It is easy to see that this leads to a dispersion proportional to k^2, in agreement with general arguments[41] for Hamiltonians with the detailed balance property. These findings seem consistent with the notion that the HR state can be thought of as a critical state between the strong and weak pairing phase of a d-wave superconductor of composite fermions.[16] The implication of gapless excitations in the thin torus limit of the hollow core Hamiltonian is the main result of this paper.

IV. DOMAIN WALLS AND ZERO-MODE COUNTING ON THE TORUS

The zero modes of the hollow-core Hamiltonian do not only consist of the ground states at filling factor $\nu = 1/2$, but also of all states that have $2n$ quasi-hole type excitations added to a $\nu = 1/2$ liquid. We are now in a position to identify the thin torus limits of the complete set of zero modes. Enumerating the number of zero mode states for fixed particle number N and fixed n has been an integral part of the study of solvable Hamiltonians on the sphere,[24,26,42–44] where the counting is aided by the polynomial structure of the underlying wave functions. Here we will generalize some of these results to the torus. The thin torus limiting states serve as natural bookkeeping devices for this task, enabling the counting of zero modes even in the absence of a simple polynomial structure of the many-body wave functions. Note that although we make use of the simplicity of the thin torus states for the counting, the number of zero modes does not depend on the aspect ratio of the torus. Remarkably, the torus counting formulas we obtain in this way retain the structure of their counterparts for the sphere, and do not involve additional sums over topological sectors, as one might naively expect.

In the thin torus limit, quasi-holes manifest themselves as domain walls between the various ground-state patterns.[10,12] In the $\nu = 1/2$ state, the charge of elementary quasi holes is $1/4$.[18] Domain walls of this charge can be made between A- and B-type ground state patterns as shown in Fig. 4. It is clear that these domain walls avoid any energy cost from the dominant terms of the thin torus Hamiltonian as described in the preceding section. Any A-string pattern allows for the presence of a singlet pair of defects that is delocalized within the string as in an A'-type ground state, Fig. 4e). When this is the case we will continue to speak of an A'-string within the sequence of patterns. It is easy to see that the detailed balance condition remains satisfied at the boundary of such an A'- string. The reasons are similar to those discussed above for configurations as shown in the first line of Fig. 2b), where the members of the singlet defect pair as at close distance. It follows that states containing A'-strings, separated by hole-type domain walls from other permissible strings, are zero energy eigenstates of the thin torus Hamiltonian. For the same reasons, a single delocalized defect with given S_z may be embedded into an A-string, Fig. 4f), like in the odd N ground states at $\nu = 1/2$ discussed above. We will also refer to such strings as A'-strings, with the understanding that A'-strings can harbor one or two delocalized defects. To enumerate the number of zero mode states for N particles with $2n$ quasi-holes present, we thus need to count the number of all string-sequences of the form

$$ABABA'BABA'\ldots \tag{25}$$

with $2n$ domain walls, where strings can have variable lengths, including 0 (for the fusion of two domain walls at the same point, see Fig. 4b),d)), and B-strings alternate with A- or A'-strings. In the following, we will always assume $n > 0$, unless explicitly stated otherwise.

Knowing the structure of general quasi-hole states in the thin torus limit, we can count their number. We define the domain-wall position w_i, $0 \le i < 2n$ as the position of the first occupied orbital in an A, A'- or B-string,[45] Fig. 4 . We first consider only a subset of patterns that satisfy a "special boundary condition" where $w_0 = 0$ is the leading position of an A- or A'-string. Let $\Phi_0(N, n)$ be the number of such patterns for N particles

and $2n$ domain walls. The LLL then consists of $qN+n$ orbitals, with $q=2$ in the present case. We will, however, later generalize the result to $\nu=1/q$ HR states. It is easy to see that, if all patterns satisfying the special boundary condition are translated in all possible $qN+n$ ways, each viable pattern is generated exactly n times. It follows that the total number of states for N particles with $2n$ quasi-holes is

$$\Phi(N,n,q)=\frac{qN+n}{n}\,\Phi_0(N,n)\;. \tag{26}$$

To find an expression for $\Phi_0(N,n)$, let F be the total number of defects present in the A'-strings of a pattern. Let $\Phi_{0;F}(N,n)$ be the number of patterns satisfying special boundary conditions and having F defects. For each such pattern, we can consider the pattern obtained by "squeezing out" all the defects. This is then a pattern with $N-F$ particles, and the same number of domain walls, all of which are between A- and B-strings, with no A'-strings present. The number of such patterns is $\Phi_{0;0}(N-F,n)$. Conversely, to go from a pattern without defects and $N-F$ particles to one with F defects and N particles, F defects must be distributed over n A-strings. Each A-string can either harbor one defect of any spin projection, or two defects forming a singlet. Distributing the F defects over n A-strings is thus exactly the same problem as putting F spin-1/2 fermions into n available spatial orbitals. The number of ways to do this is $\left(\begin{array}{c}2n\\F\end{array}\right)$, such that

$$\Phi_{0;F}(N,n)=\left(\begin{array}{c}2n\\F\end{array}\right)\Phi_{0;0}(N-F,n)\;. \tag{27}$$

A similar combinatorial factor of $\left(\begin{array}{c}2(n-1)\\F\end{array}\right)$ appears in the same problem on the sphere.[24] The difference is owed to boundary conditions on the sphere, which, in the absence of quasi-holes at the poles, enforce the presence of A-type strings at both boundaries in the "dominance pattern" of the state. The latter might also be thought of as the ground state in a "prolate spheroid limit," where such boundary conditions should become manifest at a Hamiltonian level, in close analogy to the discussion given above for the torus.[46] In particular, this boundary condition is the reason for the non-degeneracy of the ground state at the "incompressible" filling factor on the sphere.

It thus remains to calculate $\Phi_{0;0}(N,n)$. This is straightforward. The possible domain wall positions are characterized by the conditions

$$\begin{aligned}&0=w_0\le w_1\le\ldots\le w_{2n-1}<qN+n\\&w_{2j}=w_{2j-1}+1 \mod 2q\\&w_{2j+1}=w_{2j} \mod 2q\;.\end{aligned} \tag{28}$$

These can be simplified by introducing new integers k_i via

$$w_{2j}=2qk_{2j}+j\;,\; w_{2j+1}=2qk_{2j+1}+j\;. \tag{29}$$

The only constraint on the k_i is then

$$0=k_0\le k_1\le k_2\le\ldots\le k_{2n-1}\le\frac{N}{2}\,. \tag{30}$$

The number of possibilities to satisfy this constraint is just the number of (weak) compositions of $N/2$ into $2n$ parts, and is thus

$$\Phi_{0;0}(N,n)=\left(\begin{array}{c}N/2+2n-1\\2n-1\end{array}\right)\;. \tag{31}$$

Putting together Eqs. (27), (31) , summing over all relevant values of F and plugging into Eq. (26) gives

$$\Phi_{\rm HR,torus}(N,n,q)=\\ \frac{qN+n}{n}\sum_{F,\,F=N \bmod 2}\left(\begin{array}{c}2n\\F\end{array}\right)\left(\begin{array}{c}(N-F)/2+2n-1\\2n-1\end{array}\right)\;. \tag{32}$$

This result is also valid for HR states at general filing factor $\nu=1/q$, $q\ge 2$. For this we only need to observe that the unit cells for the A- and B-patterns become

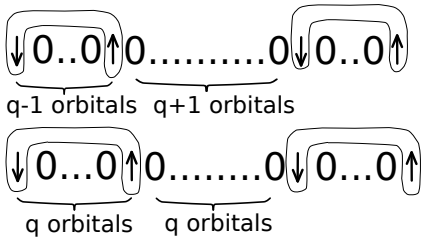

(33)

at general q, which easily follows from a generalization of the calculation presented in the preceding sections, where q replaces the exponent 2 in the Laughlin-Jastrow factor. A'-strings likewise consist of delocalized charge neutral defects inside an A-pattern, subject to analogous rules. Only Eq. (26) depends on q, and the validity of its generalization to general q is obvious.

One may also be interested in the number of the zero-mode multiplets of given total spin S, for given n, N, q. It is clear that this can be answered similarly, through a straightforward replacement of the combinatorial factor in Eq. (27) by that corresponding to the number of spin S-representations in a system of F spin-1/2 fermions with access to n states.

With the "special" boundary condition replaced by the boundary conditions for the sphere that we identified above, the same method yields[47]

$$\Phi_{\rm HR,sphere}(N,n)=\\ \sum_{F,\,F=N \bmod 2}\left(\begin{array}{c}2(n-1)\\F\end{array}\right)\Phi_{0;0}(N-F,n+1/2)\;, \tag{34}$$

in agreement with Ref. 24. This may serve as some confirmation that the matrix elements of the thin torus Hamiltonian have been identified correctly. Note that

the torus result (32) explicitly depends on q, whereas the one for the sphere does not.

The strategy for zero mode counting presented here can be effortlessly generalized various other paired and related quantum Hall states.[48] E.g., for the Moore-Read (MR) sequence of states, we can again distinguish two basic kinds of strings, which may be separated by domain walls in the thin torus limit of zero mode states.[11,13,49] One type of string must always contain an even number of particles, whereas the other may be even or odd in length. At $\nu = 1/2$, e.g., we have $11001100\ldots$, and $10101010\ldots$,[13] with the latter type of string being able to contain an odd number of particles. This even/oddness can again be associated with a fermionic degree of freedom.[50] A calculation highly analogous to that carried out above for HR states yields

$$\Phi_{\mathrm{MR,torus}}(N,n,q) = \frac{qN+n}{n} \sum_{F,\, F=N \bmod 2} \binom{n}{F} \binom{(N-F)/2+2n-1}{2n-1} , \tag{35}$$

where F corresponds to the number of spinless fermions associated with strings of odd length.[23] The change in the fermionic combinatorial factor compared to Eq. (32) reflects the fact that the fermionic degrees of freedom are now spinless. The above may again be compared to the known result for the sphere.[24]

Similarly, the MR sequence is intimately related[51] to the (331)-Halperin bilayer state.[17] Here we adopt the convention[24] to refer to the Halperin state with $m = m' = q+1$, $n = q-1$ as a (331)-state at general filling factor $1/q$, the case $q = 2$ being the proper (331)-state. In the thin torus limit,[15] the (331)-patterns can be "collapsed" onto the MR patterns by dropping the (pseudo)-spin information. At $\nu = 1/2$, one pattern is $XX00XX00\ldots$ where XX denotes an equal amplitude superposition between $\uparrow\downarrow$ and $\downarrow\uparrow$. We will refer to this pattern as "A-pattern", as it is also the pattern associated with the ground state on the sphere. This pattern collapses onto the $11001100\ldots$ MR pattern, and combinatorially behaves in the same manner. The other MR-pattern is descended in the same way from what we will call the "B-pattern" of the (331)-state

$$\uparrow 0 \downarrow 0 \uparrow 0 \downarrow 0 \ldots \uparrow 0 \downarrow . \tag{36}$$

Here, we insist on the leading spin being $\uparrow$, and the final one being $\downarrow$. More generally, we can of course add a sequence $\downarrow 0$ at the left end, and/or a sequence $0 \uparrow$ at the right end. These we can think of as the insertion of an up-spin and/or down-spin fermion into a "state" provided by each B-string. This then exactly reproduces the counting for the HR state, and we find that[52]

$$\Phi_{(331),\mathrm{torus}}(N,n,q) = \Phi_{\mathrm{HR,torus}}(N,n,q) . \tag{37}$$

We emphasize that this identity does not quite hold for the sphere,[24] which is chiefly due to the exchanged roles between A- and B-patterns with regard to harboring the spin-1/2 fermions. On the torus, however, this exchange of roles is inconsequential. We also note that Eq. (37) does not hold for $n = 0$. This is so because we can distinguish B-strings with 0 and 2 fermions only for B-strings that terminate in a domain wall. For $n = 0$, Periodic boundary conditions on the torus prevent this distinction.

For the (331)-state we could also ask for the number of zero-modes with given value of the total S_z. Again, this amounts to a trivial replacement of the fermion combinatorial factor in Eq. (32). The general relation Eq. (37) between the (331) and HR counting also carries over to sub-sectors of given total S_z. Unlike for the HR case, however, the total spin S is a priori not-well defined for the (331)-zero modes.

Finally, close connections between the HR state and the Haffnian[19,25] have recently been observed.[37] There, a scheme has been proposed to map the HR counting problem onto that of the Haffnian, by dressing the latter with spin according to certain rules. In the present context, it is more natural to proceed along the reverse direction, which allows us to obtain an explicit Haffnian torus counting formula. This can be done by applying the results obtained for the HR case to the Haffnian by "dropping" the spin degree of freedom. More precisely, we assume that the matrix elements in the thin torus limit of the Haffnian parent Hamiltonian[25] are the same as in the HR case, except that there is no analogue of the penalty for two particles to be at distance 2 or less, if they form a triplet state. With this rule dropped, it is easy to see that now there is no limit to the number of delocalized spinless defects that can be immersed into the (now spin collapsed) A-pattern. These defects should hence be thought of as spinless bosons. Making the proper adjustments to Eq. (34) reproduces the Haffnian counting on the sphere,[25] and making similar adjustments to Eq. (32) yields

$$\Phi_{\mathrm{Haff,torus}}(N,n,q) = \frac{qN+n}{n} \sum_{\substack{B \\ B=N \bmod 2}} \binom{B+n-1}{n-1} \binom{(N-B)/2+2n-1}{2n-1} . \tag{38}$$

This agrees with the data published in Ref. 37. Again, this is valid for $n > 0$. For $n = 0$, the non-trivial Haffnian torus degeneracy can be treated separately,[53] and has been discussed from the point of view of dominance patterns recently.[37]

V. DISCUSSION

In this work, we have analyzed the thin torus limit of the Haldane-Rezayi state, by first analyzing the behavior of the ground state wave functions, and inferring the dominant matrix elements of the thin torus hollow-core

Hamiltonian. The latter were constructed to be consistent with the uniqueness of the ten zero energy ground states at filling factor 1/2, and with the necessary locality of the thin torus Hamiltonian. From there we were able to deduce the existence of both singlet and triplet gapless excitations in the thin torus limit. Assuming adiabatic continuity of the low energy sector between the thin torus and the 2D limit, the existence of gapless excitations in the HR state follows, in agreement with general arguments.[5,6,9] So far the notion of adiabatic continuity has been mainly studied in cases where an energy gap is believed to exist in the 2D regime, in agreement with the thin torus limit.[10–13] The findings made here do, however, have much in common with our earlier analysis of a critical point between the (331)-state and the MR state, using the thin torus approach.[15] There we found gapless excitations in the thin torus limit at a critical point, within one topological sector of the thin torus theory, but not in others. We note that even in the fully gapped case, the excitation spectrum within different topological sectors is generally not identical in the thin torus limit. This is so because these sectors become locally distinguishable in this limit, and need not be related by any symmetry. Indeed, the ground state degeneracy itself could be lifted by a local perturbation away from the special solvable point. These spectral differences all disappear when we leave the thin torus limit and cross over into the 2D regime. For these reasons we argued in Ref. 15 that gapless states may generically reveal their gapless excitations in the $L_y \to 0$ limit of some topological sectors, but not of others. The present analysis strengthens this case, in particular because the same observations could be made for a solvable Hamiltonian, whereas in Ref. 15 we had to move away from the solvable point.

A small point worth mentioning is the fact that even though the B-type states do not seem to couple locally to gapless excitations when the $L_y \to 0$ limit is taken, they do so in the "dual" limit $L_x \to 0$ of the torus. In particular, a certain linear combination of B-ground states (i.e., states approaching B-patterns in the $L_y \to 0$ limit) will approach A-type patterns in this dual limit (cf. Ref. 54). It is thus true that each of the states in Eq. (1) locally couples to gapless excitation in at least one of the two mutually dual limits. This somewhat removes the inequivalence between sectors that exists when the $L_y \to 0$ limit is considered by itself.

Despite these subtleties, we argue that the presence of gapless excitations in the thin torus limit can actually be a stronger indication for the nature of the 2D limit than the absence of such excitations. To make this case, we consider a cylinder with $L_x = \infty$ and finite L_y. If there are gapless excitations in the $L_y \to 0$ limit, a sufficient assumption is that for any finite L_y, the properties of the system are analytic in L_y. This seems reasonable for the "special" solvable Hamiltonians. However, if there are gapless excitations at any value of L_y, they exist by definition in the limit $L_y \to \infty$, so long as this limit is well-defined. The converse, however, is not true. Having an energy gap for any finite value of L_y does not necessarily prevent this gap from closing as the limit $L_y \to \infty$ is taken.[55] The assumption of analyticity in L_y, while still subject to detailed justification, is thus more powerful when gapless excitations are identified in the thin torus/cylinder limit.

We close this section with some comments on possible generalizations to other states, such as the gaffnian.[8] In general, we expect that the existence of gapless excitations cannot be inferred from the knowledge of the thin torus patterns alone. Instead it requires the detailed study of a given parent Hamiltonian. It is likely a special feature of the HR state that the complete set of thin torus patterns already contains enough information about the parent Hamiltonian such that the existence of gapless excitations can be concluded (in the thin torus limit). While in general, a more direct analysis of the parent Hamiltonian is necessary, we are encouraged to believe that such an analysis is not only technically possible in the thin torus limit, but will yield results that are qualitatively correct also away from this limit.

In this context, it may be of interest that various families of states have been discussed in the literature[56,57] that were proposed to have the same patterns of zeros (as defined in Ref. 29). In particular, the family of S_3 states[57] includes both unitary and non-unitary wave functions, and parent Hamiltonians for both kinds have been proposed. Two states in this infinite family can, in general, be distinguished by their torus degeneracy, which presumably can become arbitrary large. At the same time, at the incompressible filling factor $\nu = 3/4$ there exist only 20 thin torus patterns that satisfy the generalized Pauli principle (GPP) associated with the patterns of zeros (no more than 3 particles in any 4 adacent orbitals). For an S_3 state whose torus degeneracy $D \leq 20$, we expect the thin torus limits of the ground states to be some subset of these 20 patterns. On the other hand, for $D > 20$ it is necessarily possible to form linear combinations of ground states that become orthogonal to these 20 patterns in the thin torus limit. The thin torus limits of such states will be more complicated, and will violate the GPP. This may happen, e.g., in much the same manner in which our A' states violate the GPP enforced by the diagonal matrix elements in the thin torus limit. For these reasons, we find it not unlikely that thin torus limits, taken for a complete orthogonal set of torus ground states, may still distinguish different members of the S_3 family of states. In particular, we see no obvious reasons why the adiabatic continuity conjecture must fail in those cases where a suitable parent Hamiltonian does exist. Though complicated thin torus limits may appear, the case of the HR state presented here suggests that such limits still contain valuable information. We believe that a detailed investigation of the utility of the present approach to the S_3 states would be interesting, and leave this possibility for future study.

VI. CONCLUSION

We have constructed the thin torus picture of the Haldane-Rezayi state, and found the existence of gapless excitations in this limit. This provides some further evidence in favor of the conjectured gapless nature of this state. We have also used our results to derive, for the first time, zero mode counting formulas for the special Hamiltonian of the HR state –and several others– on the torus. The observations made here in the thin torus limit may serve to guide a more rigorous proof of the gapless nature of the HR state. For this one would need to identify wave function expressions that analytically continue the gapless excitations found here, say, to a torus of arbitrary size and aspect ratio. We leave this exciting possibility for future work.

ACKNOWLEDGMENTS

We are indebted to E. Ardonne, N. Read, E. Rezayi, and S. Simon for insightful discussions. AS would like to thank R. Thomale for helpful comments on the manuscript. This work was supported by the National Science Foundation under NSF Grant No. DMR-0907793 (AS) and NSF Grant No. DMR-1004545 (KY).

Appendix A: The structure of the p-matrix

In this and the following appendices, we present the remaining details in the calculation of the thin cylinder limits of the HR ground states. We first proof that the matrix $p_{\alpha\beta}$ that leads to the maximum of Eq. (4) is always of the form (8). To this end, we plug Eq. (5) into Eq. (4), obtaining

$$S = \text{const} + \sum_{\alpha,\beta,\gamma} \left(p_{\alpha\beta} p_{\alpha\gamma} + p_{\alpha\beta} m_{\alpha\gamma} + p_{\alpha\gamma} m_{\alpha\beta} \right) . \quad \text{(A1)}$$

For fixed indices α, β, we extract the dependence of S on the matrix element $p_{\alpha\beta} = -p_{\beta\alpha}$ via

$$S = 2(p_{\alpha\beta}^2 + p_{\alpha\beta} r_{\alpha\beta}) + \text{const} \ , \quad \text{(A2)}$$

where the constant and $r_{\alpha\beta}$ depend on other matrix elements of the p-matrix, but not on $p_{\alpha\beta}$, and

$$r_{\alpha\beta} = \sum_{\gamma,\gamma\neq\beta} (p_{\alpha\gamma} + m_{\alpha\gamma}) - \sum_{\gamma,\gamma\neq\alpha} (p_{\beta\gamma} + m_{\beta\gamma}) . \quad \text{(A3)}$$

It is clear from the quadratic structure of Eq. (A2) that for any p-matrix that maximizes S, $|p_{\alpha\beta}|$ must take on the maximum possible value $m_{\alpha\beta}$. For otherwise, the value of S could certainly be increased. More precisely, it follows that

$$p_{\alpha\beta} = m_{\alpha\beta} \, \text{sign}(r_{\alpha\beta}) \ , \quad \text{(A4)}$$

unless it happens that $r_{\alpha\beta} = 0$, in which case either sign of $p_{\alpha\beta}$ is possible. In either case, $\tilde{r}_{\alpha\beta} = r_{\alpha\beta} + 2p_{\alpha\beta}$ is certainly non-zero so long as $|p_{\alpha\beta}| = m_{\alpha\beta}$ is non-zero, and we always have

$$p_{\alpha\beta} = m_{\alpha\beta} \, \text{sign}(\tilde{r}_{\alpha\beta}) . \quad \text{(A5)}$$

From Eq. (A3), we also have

$$\tilde{r}_{\alpha\beta} = r_\alpha - r_\beta \ , \quad \text{(A6)}$$

where

$$r_\alpha = \sum_\gamma (p_{\alpha\gamma} + m_{\alpha\gamma}) \ . \quad \text{(A7)}$$

There is a permutation ρ of N objects such that $r_\alpha \leq r_\beta$ for $\rho_\alpha < \rho_\beta$, where equality of r_α and r_β can, by construction, only hold for $m_{\alpha\beta} = 0$. For such a permutation, we then have

$$p_{\alpha\beta} \ = m_{\alpha\beta} \, \text{sign}(\rho_\alpha - \rho_\beta) \ , \quad \text{(A8)}$$

which is Eq. (8). We have thus shown that this equation must hold for any p-matrix that leads to a maximum of S, for some permutation ρ. As explained in the main text, ρ can be thought of as giving rise to an arrangement of particles on a "squeezed lattice".

Appendix B: The squeezed lattice: Effective Coulomb interaction

The proper choice of ρ depends on the symmetric matrix $m_{\alpha\beta}$, which depends both on the state and on the "pairing permutation" σ under consideration, as defined in the main text, Eqs. (6), (12). Here we show that the proper choice of ρ, i.e. the arrangement of the particles on the squeezed lattice, is obtained by minimizing an energy due to an effective attractive "Coulomb interaction" between members of a pair. To see this, we first observe that in the second term of Eq. (A2), the sum over γ gives rise to the α-independent constant $\sum_\gamma m_{\alpha\beta}$, such that the term vanishes after summing over α and β by symmetry. For the same reasons, the third term vanishes as well. In we did not use this fact in Appendix A, since its present form, the argument given there can be used in more general situations where $\sum_\gamma m_{\alpha\beta}$ depends on α. This is the case, e.g., in Ref. 15. For the first term of Eq. (A2), we plug in a general relation of the form (22) :

$$S = \sum_{\alpha\beta\gamma} s_{\alpha\beta} s_{\alpha\gamma} \, \text{sign}(\rho_\alpha - \rho_\beta) \text{sign}(\rho_\alpha - \rho_\gamma) + \text{const} . \quad \text{(B1)}$$

According to Eq. (A8), for the A- and B-states, the s-matrix is just the m-matrix defined in Eqs. (6) and (12). Here we will consider a slightly more general problem, of which these equations are special cases. Consider a pairing of N indices, where we denote the partner of the

index α by $\overline{\alpha}$, such that $\overline{\overline{\alpha}} = \alpha$. Consider then a symmetric matrix $s_{\alpha\beta}$ defined as

$$\begin{aligned} s_{\alpha\beta} &= 0 \quad \text{for } \alpha = \beta \\ s_{\alpha\beta} \equiv s_\alpha &= s_{\overline{\alpha}} \quad \text{for } \beta = \overline{\alpha} \\ s_{\alpha\beta} &= s \quad \text{otherwise.} \end{aligned} \tag{B2}$$

Plugging this into Eq. (B2) yields, after some amount of straightforward calculation:

$$-S = 2\sum_\alpha s(s - s_\alpha)|\rho_\alpha - \rho_{\overline{\alpha}}| + \text{const.} \tag{B3}$$

In the A- and B-state, s_α is a constant, and the coefficient $s(s - s_\alpha)$ is positive (cf. Eqs. (6), (12)). Note also that ρ_α and $\rho_{\overline{\alpha}}$ are the positions of a pair on the squeezed lattice. We can thus interpret Eq. (B3) as the total energy of particles on the squeezed lattice where pairs interact via an attractive linear 1D Coulomb potential. Clearly, minimization of this energy requires one to place members of a pair onto adjacent sites of the squeezed lattice, as shown in Eq. (9). For the A- and B-states, this then has the implications stated in the main text.

The above observations are now easily extended to the A'-states. The structure of the s-matrix was worked out in the main text, Eq. (23). Recall that a single pair has been excluded from the pairing $\mathcal{P}$. Eq. (23) is then another special case of Eq. (B2), with $s_\alpha = 0$ for all except one pair of indices, for which $s_\alpha = s_{\overline{\alpha}} = 1 = s$. The implications of this are plainly apparent in Eq. (B3). All pairs attract in the same manner as before, except for the special "broken" pair, whose Coulomb attraction has now been switched off. The position of the members of the broken pair on the squeezed lattice are then arbitrary; they all lead to the same maximum value of S. All the other pairs must still be nearest neighbors on the squeezed lattice. The resulting "un-squeezed" thin cylinder state is the equal amplitude superposition described in the bulk of the paper.

The present method to work out the thin torus patterns of the Haldane-Rezayi state can be used for other paired states as well. In particular, it applies almost without change to Moore-Read states. This, in addition to the similar structures of the counting rules found here and in Ref. 24, is another manifestation of various formal connections between these states.

Appendix C: Coefficient of the dominant terms in the A'-state polynomial

Here we calculate the coefficient of the dominant monomials in the A'-state thin cylinder limit, as identified in the preceding appendix. These monomials correspond to a p-matrix of the form defined in Eqs. (22), (23). In particular, this will prove that these coefficients are non-zero. Recall that $\mathcal{P}$ in Eq. (23) is a pairing of the particle indices into $N-1$ pairs, with one pair left out. The permutation ρ must give rise to a squeezed lattice configuration with all pairs in $\mathcal{P}$ nearest neighbors. This is necessary to maximize S, and hence the κ-dependent part of the amplitude (3), as shown in Appendix B. All monomials corresponding to a p-matrix satisfying these rules can be obtained only from this particular p-matrix. This is so because other p-matrices satisfying these rules will either permute particle indices with like spins (which for fermions, must always lead to a different monomial). Or, in general, other such p-matrices lead to different states with the "defect" particles occurring in the A'-pattern in different positions. On the other hand, p-matrices not satisfying the rules above will either lead to monomials with vanishing coefficients, or to ones with lower S. For these reasons, we only need to focus on a particular p-matrix satisfying the rules summarized here, and calculate the coefficient of the monomial obtained by choosing the term $\xi_\alpha^{m_{\alpha\beta}+p_{\alpha\beta}}\ \xi_\beta^{m_{\alpha\beta}-p_{\alpha\beta}}$ in factors depending on ξ_α and ξ_β in Eq. (16). It is easy to see that all such p-matrices lead to a coefficient of the same value, up to a sign. We thus choose the pairing of up-spin and down-spin indices given by

$$\mathcal{P} = \{(2\downarrow, 2\uparrow), (3\downarrow, 3\uparrow)\ldots(N'\downarrow, N'\uparrow)\}\,, \tag{C1}$$

where we write $N' = N/2$ for convenience, and the pair $(1\uparrow, 1\downarrow)$ is left out. This defines an s-matrix according to Eq. (23). We also choose a squeezed lattice configuration, ρ, consistent with this pairing (App. B), and define $p_{\alpha\beta}$ from Eq. (22).

Now we first fix the permutations σ, λ in Eq. (16), and generate a monomial using the p-matrix from the resulting polynomial of the form (17), where the signs depend on σ and λ. The coefficient of the resulting monomial is of the form

$$(-2)^{N'-1}\chi(\sigma,\lambda)\,, \tag{C2}$$

where the first term indicates that $N'-1$ of the mixed terms $\xi_\alpha\xi_\beta$ are chosen, one for each pair in $\mathcal{P}$, except that not all of them have a coefficient -2. Instead, some contribute $+2$, and this change of sign is accounted for in the factor

$$\chi(\sigma,\lambda) = (-1)^{\sigma+\lambda}(-1)^{g(\sigma,\lambda)}\,, \tag{C3}$$

where

$$g(\sigma,\lambda)\sum_{r=2}^{N'}\delta_{\sigma_r,\lambda_r}(1-\delta_{\sigma_r,1})\,. \tag{C4}$$

is just the number of pairs $(\sigma_r\downarrow, \lambda_r\uparrow)$ with $r>1$ that are contained in $\mathcal{P}$. The full coefficient of the resulting monomial then satisfies:

$$C_{\{n_\alpha\}} = (-2)^{N'-1}\sum_{\sigma,\lambda\in S_{N'}}\chi(\sigma,\lambda)\,. \tag{C5}$$

To evaluate this, we represent $\chi(\sigma,\lambda)$ through a binomial sum:

$$\chi(\sigma,\lambda) = \sum_{n=0}^{N'-1}(-2)^n\,\chi_n(\sigma,\lambda)\,, \tag{C6}$$

where

$$\chi_n(\sigma,\lambda) = (-1)^{\sigma+\lambda} \begin{pmatrix} g(\sigma,\lambda) \\ n \end{pmatrix} . \qquad \text{(C7)}$$

This is obtained from Eq. (C3) by simply applying the binomial theorem to $(-1)^g = (1-2)^g$, and observing that $g(\sigma,\lambda) \leq N'-1$. The point of doing this is that one may see that

$$\sum_{\sigma,\lambda\in S_{N'}} \chi_n(\sigma,\lambda) = 0 \text{ for } n < N'-1 . \qquad \text{(C8)}$$

To see this, we cast Eq. (C7) in the form

$$\chi_n(\sigma,\lambda) = (-1)^{\sigma+\lambda} \sum_{\substack{\omega\in 2^\Gamma \\ |\omega|=n}} \prod_{r\in\omega} \delta_{\sigma_r,\lambda_r} , \qquad \text{(C9)}$$

where $\Gamma = \{2,3,\ldots,N'\}$, 2^Γ is the set of all subsets of Γ, and the sum is over all subsets ω with n elements. Clearly for given σ, λ there are $\begin{pmatrix} g(\sigma,\lambda) \\ n \end{pmatrix}$ distinct choices for ω that contribute to the sum. However, for ω *fixed* and $n < N'-1$ we may consider defining a new permutation $\tilde{\sigma}$ obtained from σ by exchanging the values of σ_{r_1}, σ_{r_2} for the smallest two indices r_1, r_2 that are *not* contained in ω. It is clear that when summing Eq. (C7) over σ, terms with given ω and σ, $\tilde{\sigma}$ so related will cancel. Thus Eq. (C8) follows. Eqs. (C3) and (C8) in Eq. (C5) yield

$$C_{\{n_\alpha\}} = (-2)^{2N'-2} \sum_{\sigma,\lambda\in S_{N'}} \chi_{N'-1}(\sigma,\lambda) . \qquad \text{(C10)}$$

By definition of $\chi_{N'-1}(\sigma,\lambda)$, however, the pairs σ, λ contributing to this last sum are exactly those with $\sigma = \lambda$ and $\sigma_1 = \lambda_1 = 1$. There are $(N'-1)!$ such pairs. This gives

$$C_{\{n_\alpha\}} = 2^{N-2}(N/2-1)! \qquad \text{(C11)}$$

as stated in the main text, which is non-zero.

[1] R. B. Laughlin, Phys. Rev. Lett. **50**, 1395 (1983).
[2] G. Moore and N. Read, Nucl. Phys. B **360**, 362 (1991).
[3] C. Nayak and F. Wilczek, Nucl. Phys. B. **479**, 529 (1996).
[4] V. Gurarie and C. Nayak, Nuclear Physics B **506**, 685 (1997).
[5] N. Read, Phys. Rev. B **79**, 045308 (2009).
[6] N. Read, arXiv:0807.3107 (2008).
[7] P. Bonderson, V. Gurarie, and C. Nayak, Phys. Rev. B **83**, 075303 (2011).
[8] S. H. Simon, E. H. Rezayi, N. R. Cooper, and I. Berdnikov, Phys. Rev. B **75**, 075317 (2007).
[9] N. Read, Phys. Rev. B **79**, 245304 (2009).
[10] A. Seidel, H. Fu, D.-H. Lee, J. M. Leinaas, and J. E. Moore, Phys. Rev. Lett. **95**, 266405 (2005).
[11] A. Seidel and D.-H. Lee, Phys. Rev. Lett. **97**, 056804 (2006).
[12] E. J. Bergholtz and A. Karlhede, J. Stat. Mech. **L04001** (2006).
[13] E. J. Bergholtz, J. Kailasvuori, E. Wikberg, T. H. Hansson, and A. Karlhede, Phys. Rev. B **74**, 081308(R) (2006).
[14] E. J. Bergholtz and A. Karlhede, Phys. Rev. Lett. **94**, 026802 (2005).
[15] A. Seidel and K. Yang, Phys. Rev. Lett. **101**, 036804 (2008).
[16] N. Read and D. Green, Phys. Rev. B **61**, 10267 (2000).
[17] B. I. Halperin, Helv. Phys. Acta. **56**, 75 (1983).
[18] F. D. M. Haldane and E. H. Rezayi, Phys. Rev. Lett. **60**, 956 (1988).
[19] X.-G. Wen and Y.-S. Wu, Nuclear Physics B **419**, 455 (1994).
[20] M. Milovanović and N. Read, Phys. Rev. B **53**, 13559 (1996).
[21] V. Gurarie, M. Flohr, and C. Nayak, Nuclear Physics B **498**, 513 (1997).
[22] A. Seidel and D.-H. Lee, Phys. Rev. B **76**, 155101 (2007).
[23] A. Seidel, Phys. Rev. Lett. **101**, 196802 (2008).
[24] N. Read and E. Rezayi, Phys. Rev. B **54**, 16864 (1996).
[25] D. Green, *Strongly Correlated States in Low Dimensions*, Ph.D. thesis, Yale University, New Haven (2001), http://arxiv.org/abs/cond-mat/0202455.
[26] N. Read, Phys. Rev. B **73**, 245334 (2006).
[27] B. A. Bernevig and F. D. M. Haldane, Phys. Rev. Lett. **100**, 246802 (2008).
[28] B. A. Bernevig and F. D. M. Haldane, Phys. Rev. B **77**, 184502 (2008).
[29] X.-G. Wen and Z. Wang, Phys. Rev. B **77**, 235108 (2008).
[30] X.-G. Wen and Z. Wang, Phys. Rev. B **78**, 155109 (2008).
[31] M. Barkeshli and X.-G. Wen, Phys. Rev. B **82**, 233301 (2010).
[32] E. Keski-Vakkuri and X.-G. Wen, Int. J. Mod. Phys. B **7** (1993).
[33] A. Seidel, (2009), talk given at KITP conference on "New Directions in Low-Dimensional Electron Systems," `http://online.kitp.ucsb.edu/online/lowdim_c09/seidel/`.
[34] A. Seidel, (2009), talk given at Nordita program on "Quantum Hall physics - Novel systems and applications," `http://agenda.albanova.se/conferenceDisplay.py?confId=1411`.
[35] E. H. Rezayi and F. D. M. Haldane, Phys. Rev. B **50**, 17199 (1994).
[36] R. Thomale, B. Estienne, N. Regnault, and B. A. Bernevig, arXiv:1010.4837 (2010).
[37] M. Hermanns, N. Regnault, B. A. Bernevig, and E. Ardonne, arXiv:1101.4978 (2011).
[38] M. V. Milovanović, T. Jolicoeur, and I. Vidanović, Phys. Rev. B **80**, 155324 (2009).
[39] Since all these monomials maximize S, $p_{\alpha\beta}$ must be of the form (8) with ρ arranging the pairs of σ into neighbors on the squeezed lattice. As explained in the text, choices for ρ that lead to different $p_{\alpha\beta}$ also lead to different monomials, related by index permutation.
[40] In general, different p-matrices could contribute to the same monomial. This, however, will not be the case for the dominant ones, as shown below.

[41] C. L. Henley, Journal of Physics: Condensed Matter **16**, S891 (2004).
[42] E. Ardonne, N. Read, E. Rezayi, and K. Schoutens, Nucl. Phys. B. **607**, 549 (2001).
[43] E. Ardonne, J. Phys. A **35**, 447 (2002).
[44] E. Ardonne, R. Kedem, and M. Stone, J. Phys. A **38**, 617 (2005).
[45] For an A'-string, this leading position is that of the first doubly occupied site when the defect particle is not at the left end of the string. It is greater by one than the left-most possible position of the defect.
[46] We are indebted to N. Read for this suggestion.
[47] The shift of n by $1/2$ in the last term reflects the fact that we no longer fix the first of the domain wall positions to be at 0.
[48] For the Laughlin $\nu = 1/q$ state on the torus, a simplified version of the argument yields $\frac{Nq+n}{n}\begin{pmatrix} N+n-1 \\ n-1 \end{pmatrix} = \frac{Nq+n}{N}\begin{pmatrix} N+n-1 \\ n \end{pmatrix}$ zero modes for N particles with $qN+n$ flux quanta. The second expression holds for $n = 0$ also.
[49] E. Ardonne, E. J. Bergholtz, J. Kailasvuori, and E. Wikberg, J. Stat. Mech. **P04016** (2008).
[50] See Ref. 23 for how this feature of the Pfaffian patterns is related to the statistics of the state.
[51] M. Greiter, X. G. Wen, and F. Wilczek, Phys. Rev. B **46**, 9586 (1992).
[52] We are indebted to E. Rezayi for performing various checks on this relation.
[53] The number of bosons that can enter an A-string is limited only by the length of that string. This leads to an extensive ground state degeneracy[58] even at $\nu = 1/2$.
[54] A. Seidel, Phys. Rev. Lett. **105**, 026802 (2010).
[55] This is precisely what we expect to happen in the B-sectors.
[56] B. Estienne, N. Regnault, and R. Santachiara, Nucl. Phys. B **824**, 539 (2010).
[57] S. H. Simon, E. H. Rezayi, and N. Regnault, Phys. Rev. B **81**, 121301(R) (2010).
[58] E. Rezayi, unpublished.